Cellulose
https://doi.org/10.1007/s10570-023-05522-z

ORIGINAL RESEARCH

Effect of fines percentage on ultrasonic dewatering of cellulose nanofibrils

Udita Ringania · Robert J. Moon · M. Saad Bhamla

Received: 16 June 2023 / Accepted: 22 September 2023

Abstract In this study, we perform a comprehensive examination of the ultrasonic dewatering of cellulose nanofibril (CNF) suspensions, with particular emphasis on the role of fines content. The production of CNFs involves mechanical fibrillation which leads to the presence of different percentages of fines (fibrils under 200 µm) in the final product. Although fines have demonstrated mechanical advantages in composite materials, they also increase water retention by the fibrils, leading to increased dewatering time and energy. We selected two distinct CNF samples with 60% and 90% fines, respectively, and subjected them to ultrasonic drying until 100 wt% CNFs is reached. We found that the 90% fines samples displayed 20% longer drying times, indicating a higher water retention capacity than the 60% fines samples due to increased hydrogen bonding sites. Both fines types exhibit a biphasic pattern in water removal, with the second phase, commencing upon the elimination of half the water, displaying similar rates regardless of the fines content. As dewatering and drying processes often induce agglomeration in CNFs, we systematically dewatered both the suspensions until concentrations of 15, 25, and 35% were achieved and then redispersed to 0.01 wt% CNF. To evaluate the stability of redispersed samples, we monitored their settling behavior and conducted UV–vis transmittance analyses. Results showed that while 60% fines samples could be redispersed in 1 min, the 90% fines samples required up to 5 min to reach a similar level of stability to their original suspensions. Notably, UV–vis transmittance values remained consistent across both the 60% and 90% fines samples and their initial suspensions, indicating a lack of significant agglomeration following redispersion. These findings provide critical insights regarding the impact of fines percentages in CNFs on dewatering duration and suspension stability during ultrasonic dewatering, contributing to improved processing strategies in industrial cellulose applications.

Keywords Ultrasounic dewatering · Dewatering · Cellulose nanofibrils · Redispersion · Cellulose fines

Supplementary Information The online version contains supplementary material available at https://doi.org/10.1007/s10570-023-05522-z.

U. Ringania · M. S. Bhamla (✉)
Chemical and Biomolecular Engineering, Georgia Tech, Atlanta, GA 30332, USA
e-mail: saadb@chbe.gatech.edu

R. J. Moon
The Forest Products Laboratory, U.S.D.A. Forest Service, Madison, WI 53726, USA

Introduction

Cellulose nanomaterials (CNMs) possess a unique set of properties that have been harnessed in a range of applications, including composite materials, biodegradable and renewable packaging, biomedical

Published online: 06 October 2023

applications, and rheology modification (Moon et al. 2011; Rebouillat and Pla 2013; Jang et al. 2015; Ghasemi 2019; Patel et al. 2019; Nigmatullin et al. 2020; Chen et al. 2021; Lai and Yu 2021). Two predominant categories of CNMs are cellulose nanocrystals (CNCs) and cellulose nanofibrils (CNFs). CNFs are characterized as complex, fibril-like particles forming extensively branched networks (Moon et al. 2023), whereas CNCs primarily display a spindle-like non-branching structure. These differences arise due to the respective manufacturing processes: mechanical fibrillation for CNFs and chemical extraction for CNCs (Moon et al. 2011; Rebouillat and Pla 2013; de Assis et al. 2018).

Mechanical fibrillation during CNF manufacturing results in the formation of fines within the suspension, the quantity and characteristics of which depend on the type and duration of fibrillation employed (Stelte and Sanadi 2009; Colson et al. 2016; Ghasemi 2019; Kelly et al. 2021). Fines are defined either as fibrils with lengths and/or fibril agglomerates with diameters < 200 µm (ISO 2014), or as fibrils capable of passing through a 76 µm diameter round hole (ISO 2012). Higher fines percentage typically correlates with greater fractions of smaller fibrils, leading to increased mechanical bridging and hydrogen bonding (facilitating network formation) within the suspension (Stelte and Sanadi 2009). This increased fines percentage has been shown to enhance strength and surface properties in pulp non-woven materials (Zambrano et al. 2020). For instance, paper hand sheets incorporating CNFs as an additive exhibited an increase in tensile index proportional to the fines percentage, reaching a plateau at approximately 77% (Johnson et al. 2016). This study also noted an increase in internal bond strength and decrease in surface roughness of hand sheets as the CNF fines percentage increased. The fines percentage has also been observed to affect the adhesive strength when CNFs is used as a sole adhesive on filter paper joints, with higher adhesion achieved for CNFs with higher fines percentage (Kelly et al. 2021). A higher fines percentage can contribute to improved packaging during web formation in papermaking, thereby reducing pore sizes and increasing resistance to air permeance through paper (Johnson et al. 2016).

Although these enhanced mechanical properties are desirable, a higher fines percentage can affect the dewatering properties of a suspension negatively, leading to increased dewatering times during wet pressing (Johnson et al. 2016; He et al. 2017). As traditional dewatering and drying processes are inherently energy-intensive (Miller et al. 2015), a higher fines percentage can contribute to increased energy consumption during the manufacturing process.

Ultrasonic dewatering offers a more energy-efficient method for water removal from CNFs, with an estimated 50% energy reduction compared to traditional spray drying (Ringania et al. 2022). Previous work has explored the influence of system parameters such as the number of transducers used and the CNF flow rate on ultrasonic dewatering efficiency, providing valuable insights for process optimization and future scale-up (Ringania et al. 2022). However, the impact of material properties, particularly fines content, on ultrasonic dewatering efficiency remains uninvestigated. Given that material properties such as fines content can significantly influence dewatering times, it is crucial to examine their potential impact on the efficiency of ultrasonic dewatering, a technique recently applied to CNM suspensions.

In this study, we explore the influence of the fines percentage in a CNF suspension on the efficiency of ultrasonic dewatering and drying. We aim to assess the role of fines content on the water retention behavior and the dewatering rate. As fibril agglomeration during dewatering can pose challenges, we conduct redispersion of the dewatered samples to evaluate the extent to which dewatering and redispersion can be achieved without inducing irreversible CNF agglomeration. We investigate the efficiency of redispersion based on parameters such as CNF fines percentage, final dewatered weight%, and redispersion time. We further assess the stability of redispersed suspensions using gravitational settling experiments and UV–visible spectrometry determining the settling time, height, and potential CNF agglomeration of the fibrils.

This study aims to provide insights into the impact of fines percentage on the ultrasonic

Table 1 Specifications of the CNF samples obtained from University of Maine

% fines	Lot #	Concentration (wt%)
60% fines	U136-K	3.4 ± 0.2
90% fines	U103	3.1 ± 0.4

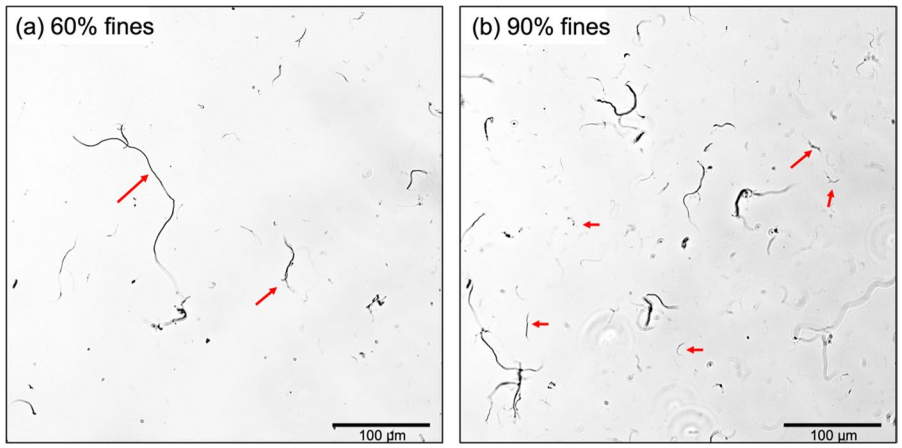

Fig. 1 Phase contrast microscopy images of CNF samples captured using optical microscope (Nikon ECLIPSE Ti2-U, using 20× objective lense and phase 1 contrats filter). The samples are at 0.01 wt% CNF diluted using DI water. Higher density of smaller fibrils observed in 90% fines as compared to the 60% fines. The red arrows point toward longer fibrils seen in 60% fines while higher density of smaller fibrils is seen in 90% fines sample

dewatering and drying process, thereby furthering our understanding of water retention based on CNF suspension parameters and optimizing the process. Additionally, our exploration into alternative dewatering processes and redispersion techniques could pave the way for innovative strategies for shipping and handling CNFs, enhancing accessibility for various industries.

Materials and methods

Cellulose nanofibers

Cellulose nanofibrils (CNFs) produced using mechanical fibrillation are provided by the Process Development Center, University of Maine, Orono (UMaine 2021). Based on the ISO specification (ISO 2014) which states 'fines' as fibrils with a length less than 200 µm, samples with 60% fines and 90% fines are used in the present work. Figure 1 shows the optical microscopy images for both fines percentages at 0.01 wt% dilution, with arrows demonstrating the difference in fibril lengths observed in both samples. These CNF suspensions have a solids content ranging between 3 and 3.5 wt%, as confirmed by oven drying experiments performed by us (with at-least 3 repeats for each). The specification of fines percentage, lot number, and solid weight content for these CNF samples are provided in Table 1.

Ultrasonic dewatering technique

The ultrasonic dewatering of CNF suspensions is achieved using a piezoelectric vibrating mesh transducer (VMT) that comprises a metal mesh connected to a piezoelectric crystal, as described in our previous study (Ringania et al. 2022). By applying voltage to the piezoelectric ceramic, high frequency vibrations in the range of the resonance frequency of the transducer (110–113 kHz) are generated in the metal mesh, which help remove water from the CNF suspension (Fig. 2a). In this work, a custom-build static ultrasonic dewatering platform as shown in Fig. 2b is used to perform two studies. (i) We dewater[1] the samples to achieve 100% CNF solid weight content (complete drying) to help understand the impact of fines percentage on water-retention by fibrils during the ultrasonic dewatering process. (ii) We dewater the as received CNF

[1] Dewatering in our work is defined as concentrating the suspension by removal of water from the system to various solid wt%.

Complete drying in our work in defined as the state of the sample when all the water has been removed from the system and the final wt. is equivalent to the solid wt. content of the initial suspension.

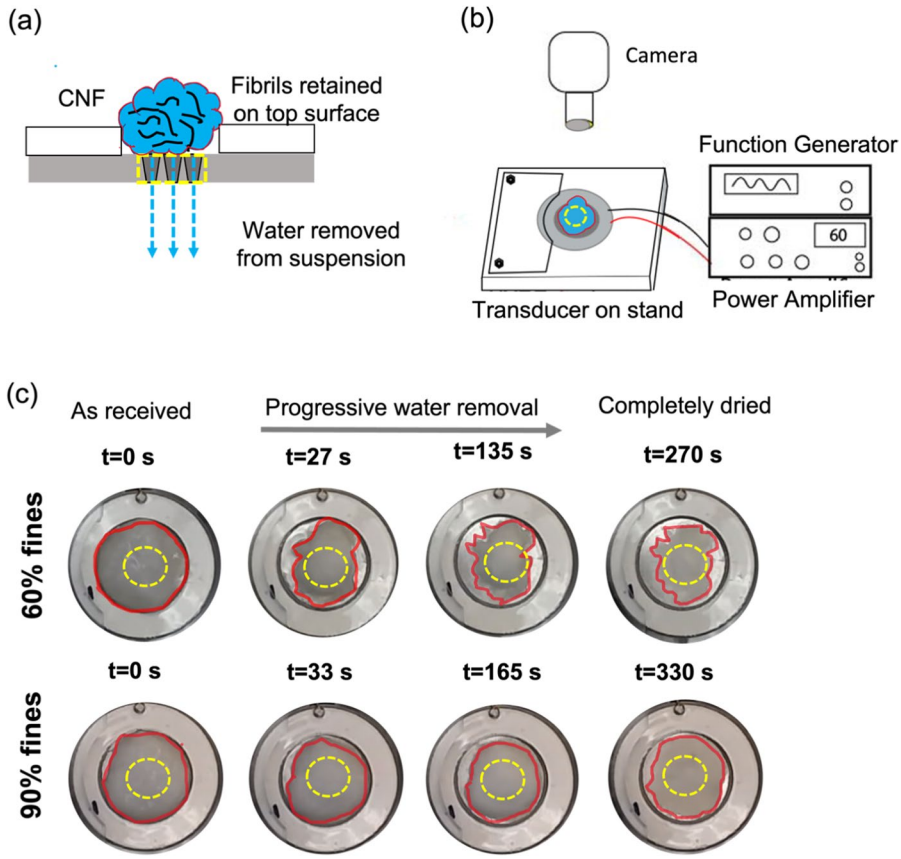

Fig. 2 **a** Schematic demonstrating the ultrasonic water removal process using a vibrating mesh transducer (VMT). High frequency vibration of the metal mesh pushes the water through the mesh leaving the fibrils behind. **b** Schematic of the static ultrasonic drying platform. **c** Timelapse of the drying process for both fines percentages at various time points. The timepoints are at 0, 0.1, 0.5 and 1 fraction of the total time taken to dry each sample. The red line depicts the CNF sample circumference as the drying process progresses with higher shrinkage observed for 60% fines. The yellow dotted circle and box represents the mesh circumference

suspension (specifications in Table 1) to various solid weight percentages: 15 wt%, 25 wt% and 35 wt% to test their subsequent redispersion and suspension stability thereby. The platform includes a horizontal transducer stand holding the VMT, which is powered by a function generator and a power amplifier. Due to the vibration-induced interference of ultrasound with the weighing system, continuous measurements of the CNFs weight are unfeasible. Therefore, we adopt interval-based weight assessments to ensure accurate data collection. First, the weight of the unconnected static VMT platform is tarred on the weighing scale. We then weigh the CNF sample (for both 60% fines and 90% fines, as received) by placing them on the VMT's metal mesh. The initial weight of the CNF suspension samples was ~200 mg. After removing from the weighing scale, we connect the VMT setup to the amplifier and initiate ultrasonic vibrations on the CNF sample. We disconnect the setup every 30 s, weighing the sample until we achieve the desired CNF wt%. At least 3 runs are conducted for each final CNF wt% for the 60 and 90% fines samples. The dewatering process was monitored and recorded using a camera (Logitech) at 2 fps, and timelapse images of the samples are shown in Fig. 2c (see SI-Movie 1, SI-Movie 2 and Online Resource 1 for details). The change in area covered by the CNFs as drying progressed is calculated through these images and presented in Online Resource 1: SI-Fig. 1.

Characterization

CNF concentration calculation

Using the initial concentration (C_i) of the CNFs in these suspensions (from Table 1), the initial weight of CNF solids ($F_i$in mg) in the sample suspension of initial weight W_i(mg) is determined:

$$F_i = \frac{C_i}{100} \times W_i \tag{1}$$

W_i can also be denoted as $W_{t=0}$ where t = 0 represents the start time point for the dewatering process.

To determine the amount of water removed between two time points, where time point represents the time elapsed from start in seconds, and assuming only water passes through the pores, we use the following formula:

$$\text{water removed between n and m time point} = W_{t=n} - W_{t=m}; \quad \text{where } n < m \tag{2}$$

where $W_{t=n}$ *and* $W_{t=m}$ indicate the weight of the sample at time n and m seconds respectively.

Finally, assuming that the solid content of CNFs in the suspension remains constant (as determined in our previous study (Ringania et al. 2022), CNF wt% at time point n is calculated by:

$$\text{CNF wt\%} = \frac{F_i}{W_n} \times 100 \tag{3}$$

Normalized weight for the samples at any given time point is calculated against the initial sample weight as below:

$$\text{Normalized weight at time point n} = \frac{W_n}{W_{t=0}} \tag{4}$$

Redispersion

The samples dewatered to different solid weight percentages (15 wt%, 25 wt%, and 35 wt%) are diluted and redispersed using deionized water to achieve a final solid weight% of 0.1% CNFs. A vortex mixer (VWR Analog Vortex Mixer No. 10153-838) operating at a speed of 8, redispersed the diluted samples in two stages. In stage I, the samples were initially redispersed for 1 min and used for gravitational settling and UV–vis transmittance experiments. In stage II, the samples were redispersed for an additional 4 min (i.e., a total of 5 min), followed by another round of gravitational settling and UV–vis transmittance experiments. As received CNFs suspensions were diluted with D.I water to 0.1 wt% CNFs by stirring for 30 s using a vortex mixer. This diluted as received CNF suspension is named "original" and was used to provide a comparison to none dewatered material.

Gravitational settling experiment

To evaluate the suspension stability of the redispersed samples compared to the original samples, we conducted gravitational settling experiments. Glass vials (20 mL total volume) containing both sets of redispersed samples (approx. 6mL in volume each), i.e., those redispersed for 1 min and total of 5 min at 0.1 wt% for both 60% fines and 90% fines, were allowed to settle for 2 and 12 h, respectively. We captured images every 5 s using a Logitech webcam to record the settling process. To quantitatively analyze the settling behavior, we calculated the height of the dispersed suspension state, characterized by the white area, using ImageJ (see Online Resource 1: SI-Fig. 2), and plotted the data against time. We used an exponential fit equation to fit the data (Online Resource 1: SI-Fig. 3, SI-Fig. 4, and SI-Fig. 5), with the asymptote y_0 representing the final settling height of the samples. We also calculated t_{90} for each sample, which is defined as the time taken to reach 90% of the final settling height.

UV–vis transmittance

Transmittance data of the redispersed suspensions for both redispersion times (1 and 5 min) along with the original suspension of 60% and 90% fines at 0.01 wt% dilution is measured using the UV/Visible spectrophotometer (Ultrospec 2100 pro). Transmittance data are recorded in reference to DI water for wavelength sweeps from 350 to 800 nm at 41 nm/s speed. At least 3 sweeps are conducted for each sample using disposable cuvettes (Fisherbrand disposable cuvette, semi-micro methacrylate cells) with path length 10 mm. Transmittance sweeps for CNF samples with various fines % (between 60% fines and 100% fines) are also recorded. All the transmission sweep data are presented in Online Resource 1: SI-Fig. 6, SI-Fig. 7, SI-Fig. 8 and SI-Fig. 9.

Results and discussion

Ultrasonic drying

We examined the influence of fines percentage on the water retention behavior of CNFs and the efficiency

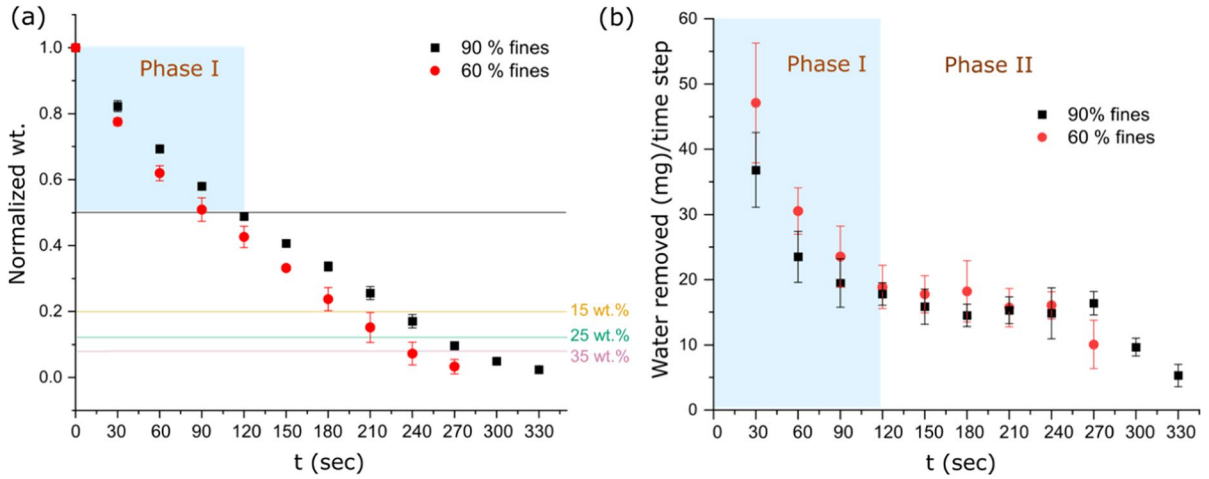

Fig. 3 **a** Normalized wt. of CNF sample, **b** water removed measured at 30 s intervals for both fines percentages as drying progressed. Two phases for water removal are observed: in phase I water removed from 60% fines is higher than 90% fines sample whereas in phase II the water removed from both fines percentage becomes similar. The shift from phase I to phase II coincides with the point when 50% of the water is removed from the system. The points when the system reaches 15 wt% (between 180 and 240 s), 25 wt% (between 210 and 270 s), and 35 wt% (between 240 and 300 s) CNFs are also marked showing the non-linearity of wt% fraction change with water removed from the system

of ultrasonic dewatering in removing water in this study. CNF suspensions with varying fines percentages were subjected to ultrasonic drying, resulting in 100% CNF solid content, and the drying process was monitored through timelapse imaging (Fig. 2c). We observed a reduction in the transducer area covered by the sample as water was removed from the system. Specifically, suspensions with 60% fines showed an area reduction of ~30%, while the 90% fines demonstrated a ~11% size reduction. This variation in area reduction provides insight into fibril packing within the sample; greater shrinkage may suggest a sparser fibril distribution in the suspension, which might lead to faster water removal from the network. Previous studies have suggested that the contact area between samples and the transducer can influence the amount of water removed from the system (Ringania et al. 2022). However, given that the mesh portion of the transducer remains covered throughout our experiments (indicated by yellow dotted circles in Fig. 2c, we assert that changes in the contact area did not impact overall water removal for both 60% fines and 90% fines samples in these investigations.

Water retention and drying times in fines suspensions

We found that the 90% fines suspensions required ~20% longer drying times compared to 60% fines suspensions to reach complete dryness. This suggests higher water retention in suspensions with larger fines percentages. The normalized weight of each sample at every time point during ultrasonic water removal is depicted in Fig. 3a. The 90% fines suspensions consistently displayed a higher normalized weight at any given time point, indicating greater water content.

Phases of water removal during ultrasonic drying

We further investigate the amount of water removed at 30-s intervals during ultrasonic drying for both samples (Fig. 3b). Our results reveal a two-phase process of water removal. Phase I, marked by greater water removal from the 60% fines suspension than from the 90% fines suspension during the initial 120 s, can be potentially explained by considering the types of water present in the system: bound, unbound and intermediate water. Bound water refers to water molecules attached to the fibrils via hydrogen bonding, while unbound water remains free and unattached. Intermediate water refers to the water molecules that

interact with the bound water but are not themselves in contact with the fibrils (Zhou et al. 2019; Xu et al. 2022). We propose that the water primarily removed in Phase I is unbound water. Given that a higher fines percentage provides more sites for hydrogen bonding, we anticipate a reduced quantity of unbound water in the system. Consequently, we observe less water removal from the 90% fines at each step compared to the 60% fines during Phase I, which results in greater water retention in the 90% fines suspension. This also accounts for the longer drying times for the 90% fines compared to the 60% fines.

Phase II commences when the amounts of water removed at each time interval for both suspensions become similar and remain consistent over time. This transition occurs between 90 and 120 s for both systems, as indicated by the 50% water removed line (in black) in Fig. 3a. We propose that as the quantity of unbound water in the systems decreases, the dewatering of the intermediate and bound water begins with intermediate water removed primarily during transition. Ultrasonic energy is primarily utilized to break the hydrogen bonds before dewatering the tightly packed fibrils. As a result, the system's dependence on the fines percentage diminishes, and water removal from both samples becomes analogous. It is important to note that quantifying the types of water in these systems falls outside the scope of this paper, and these interpretations remain speculative. Nevertheless, this understanding of water removal behavior can be crucial in designing systems specifically tailored to particular suspensions, ultimately enabling optimized water removal.

Ultrasonic dewatering

After investigating the complete water removal behavior for both fines percentages, we next explore ultrasonic dewatering to achieve various CNF wt% and their subsequent redispersion and suspension stability. Previous research has demonstrated excellent redispersion for CNF samples dewatered up to 11 wt% solids without causing irreversible CNF agglomeration (Ringania et al. 2022). Additionally, dewatering can significantly reduce water content in the system, thereby lowering shipping and handling costs without the high energy demands associated with complete water removal. Thus, dewatering is recommended for optimizing the system from both energy consumption and material integrity perspectives.

We compare samples from both 60% fines and 90% fines in terms of their redispersibility and suspension stability. The dewatering time needed to reach CNF wt% of 15, 25, and 35 wt% for both systems are shown In Fig. 3a. Subsequent dewatering experiments are conducted using these times as a reference for designing the dewatering times necessary to achieve these desired CNF wt%.

Normalized weight% versus time plots for individual samples dewatered to various weight percentages are presented in Online Resource 1: SI-Fig. 10 and SI-Fig. 11. As these data indicate, the dewatering behavior follows a similar trend to complete drying, with the 90% fines requiring longer dewatering times than the 60% fines. The time needed to reach various CNF wt% for 60% fines is shorter than for 90% fines, evidenced by the time step where the system crosses these solid weight% lines in Fig. 3(a). The nonlinear gaps between these lines, despite a constant increase in CNF wt%, are a consequence of the nonlinear relationship between CNF wt% to the amount of water removed from the system, as shown in Online Resource 1: SI-Fig. 12.

For example, when dewatering the suspensions to a CNF solid wt% of 15, 25, and 35 wt%, a change of 10 wt% solids content for each case, corresponded to a total water removal percentage from the system of 82, 92.7, and 94.2%, respectively. This shows that a much smaller amount of water removal is needed to increase the solids content from 25 wt% to 35 wt% (~ 1.5% water removed) than when going from 15 to 25 wt% (~ 10.7% water removed). Achieving CNF weight percentages between 35 and 100 wt% proved experimentally challenging due to this relationship, as the change in CNF wt% is exponential for even the slightest amount of water removed (see Online Resource 1: SI-Fig. 12). It is worth noting that if dewatering is performed to remove only 50% of the initial water, i.e., to achieve between 6 and 7 CNF wt%, the system remains in the Phase I regime alone. Whereas, for dewatering to 15, 25, and 35 wt% CNF, both water removal phases are observed.

Redispersion

The nanoscale dimensions of CNFs impart unique properties desirable for various applications, such

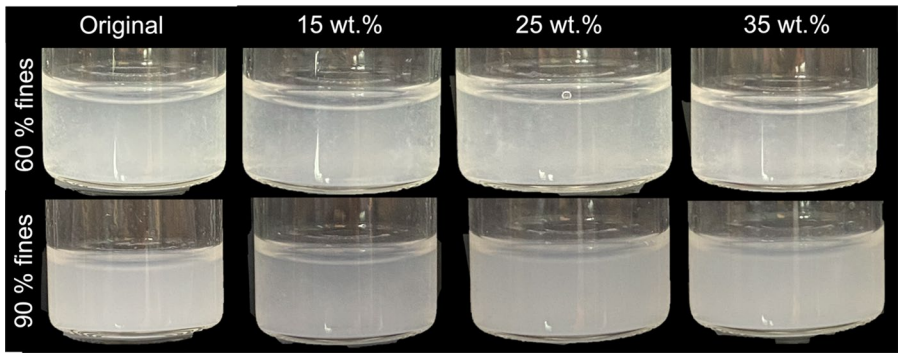

Fig. 4 Redispersed suspensions at 0.1 wt% dilutions are shown for samples dewatered to various wt% CNF along with the original sample for both fines percentages. On visual inspection, the dewatered suspesnions looked very similar to the original suspesnion with no visible agglomeration observed. Scale bar: the diamter of each beaker is 2.27 cm

as composite materials, bioproducts, and packaging, which often necessitate the use of these materials in suspension form. Therefore, dewatered and dried CNFs must be redispersed in suspension for industrial applications. However, drying and dewatering frequently lead to irreversible agglomeration of fibrils, resulting in the loss of their nanoscale dimensions and corresponding unique properties. Redispersing these agglomerated fibrils can incur high energy costs associated with breaking strong interfibrillar bonds. Consequently, it is crucial that the dewatering method does not promote significant agglomeration of fibrils and allows for successful redispersion into solution while retaining their properties (Déléris and Wallecan 2017; Posada et al. 2020).

Previous work by Ringania et al.(Ringania et al. 2022) demonstrated that samples dewatered up to 11 wt% CNFs could be successfully redispersed after 1 min of vortex mixing without any change in CNF particle morphology. As we dewater the samples to higher CNF weight percentages in this study while also varying the fines percentage, it is essential to examine the impact of these variables on redispersibility and evaluate the efficacy of the ultrasonic dewatering method. We thus redisperse the samples in two stages, i.e., 1 min followed by an additional 4 min (5 min in total), to also investigate the effect of redispersion time on redispersibility.

Figure 4 displays images of ultrasonic dewatered samples to 15 wt%, 25 wt%, and 35 wt% CNFs, for both fines percentages redispersed for 5 min and diluted to 0.1 wt%, alongside their original samples (e.g., as received CNF suspension diluted to 0.1 wt%). On initial visual inspection, we did not observe any large agglomerated fibrils, and redispersed samples appear qualitatively similar to the original samples.

While SEM and TEM are commonly employed to assess redispersion quality, these methods present inherent challenges associated with sample preparation that can induce agglomeration in fibrils. In this work, we confine ourselves to evaluations in suspension/wet state, which are more easily applicable from an industrial perspective. Therefore, besides visually inspecting the suspensions, samples are evaluated through gravitational settling experiments and UV–vis transmittance and compared to the original, never-dried samples.

Suspension stability

Achieving stable redispersed suspensions with low energy requirements is crucial for industrial applications. Suspension stability can be assessed through settling behavior, which is measured by the change in the dispersed phase's height over time. Past research has shown that suspension stability is influenced by the size of colloidal particles, where larger particles settle faster (Kumagai et al. 2019). The equilibrium height of the suspension further provides insight into its stability, with smaller height changes indicating a more stable suspension (Li et al. 2020). In our study, we evaluate suspension stability using two parameters: (a) the fractional change in height at equilibrium, and (b) the time it takes to reach 90% of the equilibrium height or t_{90}. We also consider the effect of redispersion time using these parameters.

Figure 5a, b shows the normalized change in height over time for 60% fines and 90% fines suspensions, respectively. These graphs reveal a general trend where the height change follows an exponential curve and asymptotically approaches the equilibrium height in approximately 0.5 h for 60% fines and 6 h for 90% fines. Interestingly, the 90% fines samples display a delayed settling initially, unlike their 60% counterparts, visible as an extended "tail" at the graph's start. We extract the fractional change in height at equilibrium and t_{90} from these experimental data for further analysis.

Fractional change in height (h/H) at equilibrium

To establish a baseline for these suspensions, we compare the suspension stability of the original 60% and 90% fines samples (at 0.1 wt% CNFs). Figure 5c, d illustrate the height changes for 60% fines and 90% fines, respectively. We find that the normalized change in height, h/H, for 60% fines is 0.45 ± 0.05, while it is 0.24 ± 0.03 for 90% fines. A higher height change for 60% fines implies weaker suspension stability compared to the 90% fines suspension due to the presence of higher percentage of larger fibrils. It must also be noted that the change in height of sedimentation can be impacted by the compactness of the sediment as well as the gelation point based on the flexibility and aspect ratio of the fibrils respectively (Varanasi et al. 2013; Raj et al. 2016). Higher percentage of smaller fibers may result in the formation of tighter network faster due to the presence of higher sites available for inter-molecular bonding restricting the particle movement and impacting the settling height.

As we conducted redispersion in two steps, we ran settling experiments at both stages to understand the influence of redispersion time on suspension stability. Figure 5c show the fractional change in height at equilibrium for the dewatered samples of 60% fines redispersed for 1 and 5 min. For suspensions redispersed for 1 min, we find that the equilibrium change in settling heights for the dewatered samples aligns within 1 standard deviation of the original samples' values. Two-population t-tests confirm that we cannot statistically differentiate the means of the dewatered samples from the original sample at the limit of p value < 0.05 (see Online Resource 1 for details). For the 5-min redispersion, the height change in settling for all dewatered samples stays within the statistical bounds, similar to the original sample.

yFor 90% fines, we notice that 1 min redispersion leads to a suspension with stability inferior to the original suspension. This inference is based on the higher fractional change in equilibrium height observed in the dewatered samples, as shown in Fig. 5d. When we redisperse these samples for 5 min, the suspension stability matched the original sample, as seen in Fig. 5e and confirmed by the two- population t-test (see Online Resource 1: SI-Table 2). We speculate that samples with higher fines percentages form stronger hydrogen bonds among fibrils, requiring more energy for complete redispersion compared to the 60% fines samples.

Time to reach 90% of equilibrium height: t_{90}

The 60% fines settle much more quickly compared to the 90% fines, showing t_{90} values of 0.22 ± 0.05 h and 5.06 ± 0.20 h respectively. This can be attributed to the higher percentage of fibrils in dimensions > 200 µm in the 60% fines. As larger particles settle faster, this leads to quicker settlement times to reach equilibrium, indicating lower suspension stability.

Figure 5e present the t_{90} values for all dewatered samples redispersed for 1 and 5 min for 60% fines. For 1 min redispersed samples, the t_{90} values for 15 wt% and 25 wt% samples align within 1 standard deviation of the original 60% suspension. Two-population t-tests with respect to the original suspension verify that their means are similar within the statistical limit (see Online Resource 1: SI-Table 2). However, we note that the mean for the sample dewatered to 35 wt% (redispersed for 1 min) falls outside the lower bound of 1 standard deviation of the original suspension. This suggests that the 35 wt% samples reach the equilibrium height relatively faster than the original sample. However, the two-population t-test suggests that we can still consider the means similar within the statistical limit, so we cannot definitively claim that redispersed suspension of samples dewatered to 35 wt% has poor stability.

The t_{90} values for 5-min redispersion for 60% fines samples show similar behavior to their corresponding 1-min data. Hence, a higher redispersion time does not affect the suspension settling time for the 60% fines samples. In the case of 90% fines samples,

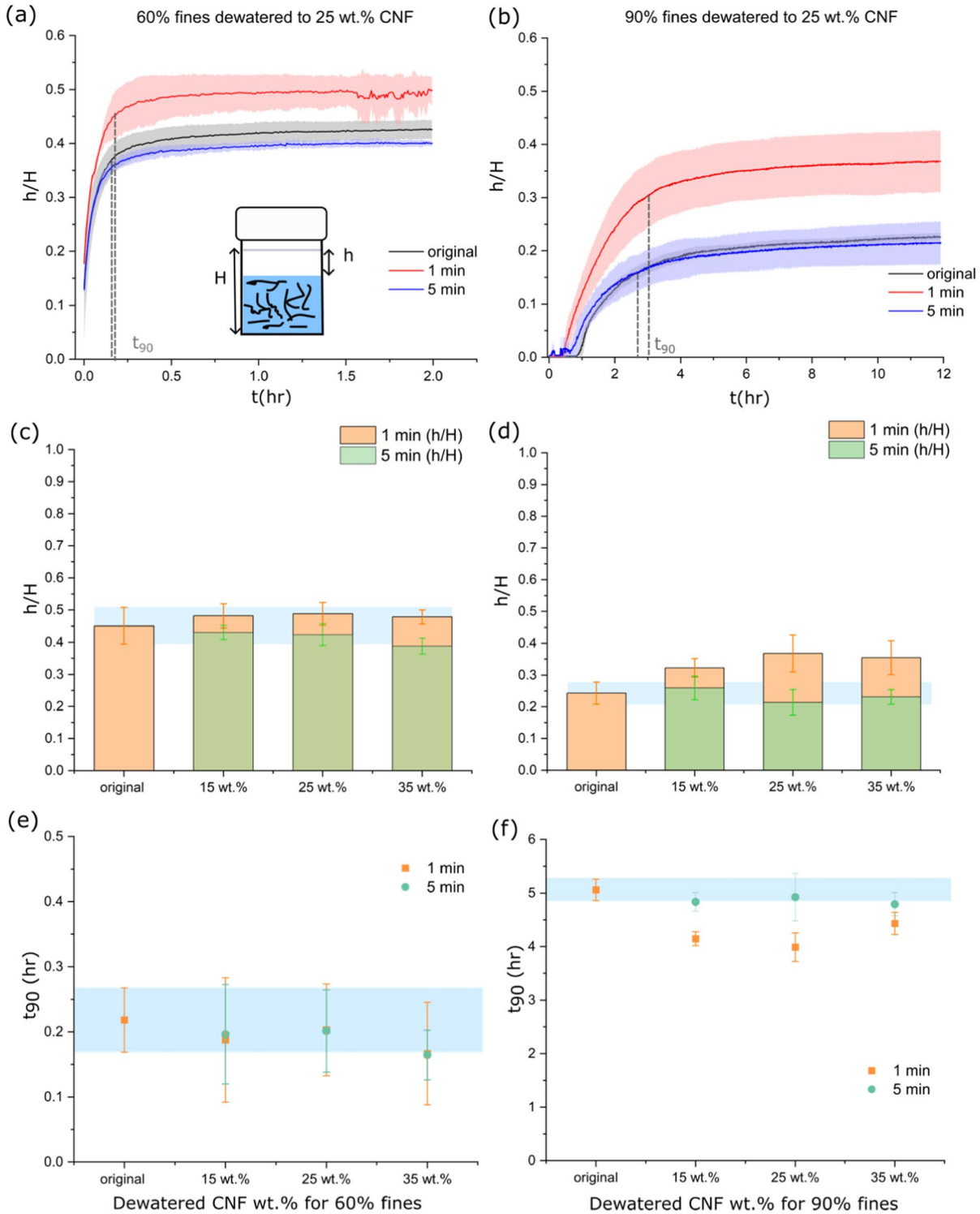
(a)
60% fines dewatered to 25 wt.% CNF
h/H
t(hr)
H
h
original
1 min
5 min
t_{90}
(b)
90% fines dewatered to 25 wt.% CNF
h/H
t(hr)
original
1 min
5 min
t_{90}
(c)
1 min (h/H)
5 min (h/H)
h/H
original
15 wt.%
25 wt.%
35 wt.%
(d)
1 min (h/H)
5 min (h/H)
h/H
original
15 wt.%
25 wt.%
35 wt.%
(e)
1 min
5 min
t90 (hr)
original
15 wt.%
25 wt.%
35 wt.%
Dewatered CNF wt.% for 60% fines
(f)
t90 (hr)
1 min
5 min
original
15 wt.%
25 wt.%
35 wt.%
Dewatered CNF wt.% for 90% fines

◂**Fig. 5** Gravitational settling experiments for samples dewatered to various wt% and redispersed for 1 and 5 min. General trend for fractional change in height of the suspension as settling progressed under gravity for the original sample compared to samples dewatered to 25 wt% CNF for **a** 60% fines, **b** 90% fines. The inset in **a** shows H: the original height of the suspension, and h: change in height of the suspension as settling progressed as depicted by the clear liquid at top. Fractional change in height at equilibrium **c** 60% fines and **d** 90% fines. Time taken to reach 90% of the equilibrium height **e** 60% fines and **f** 90% fines. The blue bar represents the standard deviation for the original data sample. The grey dotted lines represents the approximate t_{90} points

after redispersion for 1 min, the dewatered suspensions reach equilibrium height faster than the original samples. This results in lower t_{90} values for these suspensions compared to the original suspension, as shown in Fig. 5f. For samples redispersed for 5 min, we observe settling times comparable to the original sample. The t_{90} values for all dewatered samples align with the original 90% fines, as confirmed by the two-population t-test for these samples (see Online Resource 1: SI-Table 2).

Impact of redispersion time

Based on the above discussion, we note that for 60% fines, both the change in height at equilibrium and t_{90} for all dewatered samples statistically align with the original sample for both 1-min and 5-min redispersions. Thus, 1 min redispersion suffices to achieve a suspension with stability comparable to the original suspension for 60% fines. A longer redispersion time does not enhance suspension stability.

For 90% fines samples, 1 min of redispersion for all dewatered samples results in higher fractional changes of equilibrium height with lower t_{90} values, indicating inferior suspension stability to the original suspension. However, 5 min redispersion times yield statistically similar fractional changes in height at equilibrium and t_{90} for the dewatered sample suspensions, compared to the original suspension. We must note here that for samples dewatered within 10 wt%, 1 min redispersion times are sufficient to achieve stable suspensions comparable to the original suspension, as reported in our previous work (Ringania et al. 2022). Thus, for samples dewatered above 15 wt% CNFs, we recommend a 5-min redispersion to achieve stable suspensions.

UV–vis transmittance spectroscopy

UV–vis spectra are instrumental in evaluating suspension quality by assessing its transparency and opacity. The interaction between incident light and particles within a suspension—either through scattering or absorption—determines the amount of UV–vis light transmitted through the suspension. Factors such as particle size, concentration, pH, and temperature influence the UV–vis transmittance and a higher particle concentration often results in decreased light transmission (Masy and Cournil 1991). Assuming constant conditions, UV–vis transmittance spectra can help detect particle agglomerations, as they directly relate to particle width (Carr and Hermans 1978). Recent studies have used turbidity and/or UV–vis transmittance to compare the quality of CNF suspensions and films (Shimizu et al. 2016; Desmaisons et al. 2017; Sharma et al. 2021; Brännvall and Aulin 2022). We adopt this robust and fast method UV–vis transmittance method in our work to compare and detect agglomeration in redispersed dewatered suspensions with original samples. However, it is important to note that secondary absorption and scattering can obscure transmittance readings in high-concentration suspensions. Therefore, we work with low concentrations of CNFs (0.01 wt% CNFs) to avoid such complications.

To elucidate the effect of fines percentage on transmittance spectra, we first conducted wavelength sweeps on samples with various fines percentages (see Online Resource 1: SI-Fig. 6). The transmittance exhibited a wavelength-dependent increase from 350 to 800 nm. However, it must be noted that there is no linear dependence of transmittance on fines % as evidenced by the data at 550 nm, i.e., approx. midpoint of the wavelength sweep (Online Resource 1: SI-Fig. 7). The 90% fines sample had a lower transmittance than the 60% fines sample, likely due to higher particle density and morphology in the former, resulting in increased scattering (see Fig. 1). Transmittance is influenced by various system properties including particle density, size, pH, and temperature. While we might control these parameters during our experiments, differences in particle size and level of fibrillation due to varying fines percentage in our samples might significantly impact transmittance in ways beyond this study's scope. Therefore, we compare

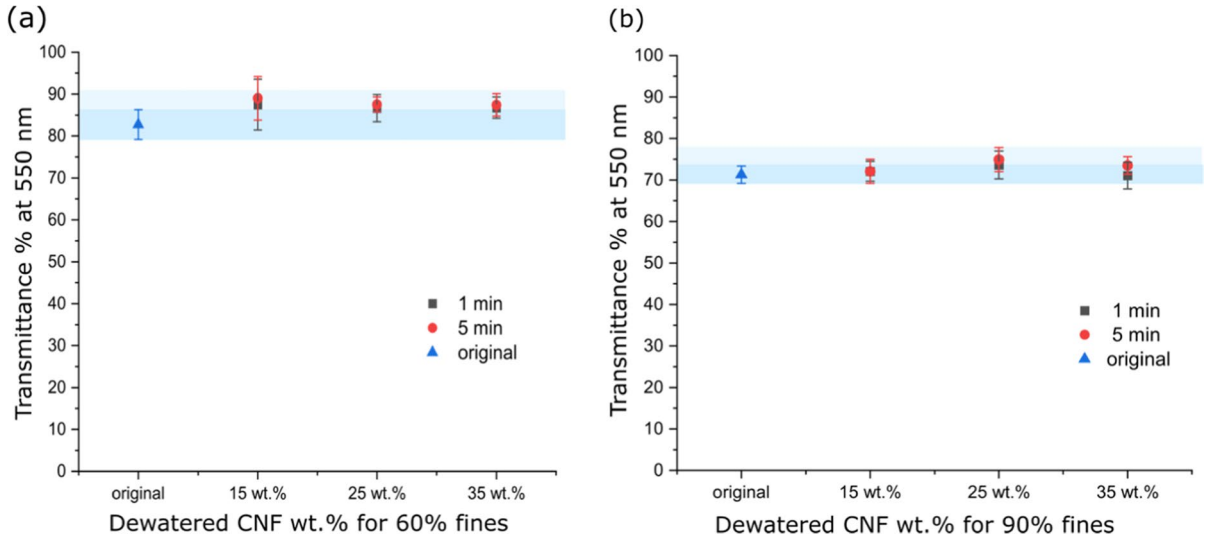

Fig. 6 UV–vis transmittance % at 550nnm wavelength for samples dewatered to various CNF wt% and redispersed for 1 min and 5 min for **a** 60% fines and **b** 90% fines along with the original suspension. All suspensions are diluted to 0.01 wt% CNF before performing the transmittance experiments. The blue bars represent the standard deviation of the original sample data

redispersed suspensions with original samples to accurately assess potential agglomeration.

We present the transmittance values at 550 nm for 60% fines samples dewatered to 15 wt%, 25 wt%, and 35 wt% CNFs, then redispersed for 1 min and 5 min are presented, in Fig. 6a. Transmittance data for wavelength sweep from 350 to 800 nm is presented in the Online Resource 1: SI-Fig. 8 and SI-Fig. 9. We observe that the transmittance for all the dewatered samples remains identical, reinforcing our earlier finding that a 1 min redispersion is sufficient for 60% fines. Statistical limits confirm the similarity in transmittance for all dewatered samples (two-population t-test in the Online Resource 1: SI-Table 2), implying no significant agglomeration and successful redispersion comparable to the original suspension.

Figure 6b shows the transmittance value at 550 nm for the 90% fines samples, dewatered to various final CNF wt% and redispersed for 1 min and 5 min. We find similar transmittance values for a given dewatered sample at both redispersion times, contrasting the different settling behavior observed at these times (two-population t-test in the Online Resource 1: SI-Table 2). Even at 1 min redispersion time, no agglomeration is triggered for dewatered samples. However, based on settling experiments, we recommend a 5 min redispersion for these samples to achieve stability similar to the original suspension. Thus, for accurate evaluation, it is recommended to perform various tests in conjunction when comparing suspension stability for redispersed samples with the original suspension.

Conclusion

This study examined the effects of fines percentage in CNFs on ultrasonic drying and dewatering efficiency using a custom-built platform. We found that the 90% fines samples took 20% longer to dry, suggesting higher water retention than the 60% fines samples. The water removal process unfolded in two phases, with the higher fines percentage suspension demonstrating lower water removal rates in the first phase due to increased hydrogen bonding sites. The water removal rate, however, became invariant with fines percentage in the second phase, when about 50% of the water was removed. We speculate this occurs because accessing higher hydrogen bonding sites becomes challenging as fibrils pack together with progressing dewatering.

Our systematic dewatering and redispersion study assessed redispersibility and suspension stability

based on settling behavior and UV–vis transmittance. We took as-received suspensions of both 60% and 90% fines, dewatered them to 15, 25, and 35 CNF wt%, and redispersed them to 0.01 wt% CNFs. Our results showed a difference in the normalized change in height for 60% and 90% fines suspensions, indicating varying suspension stability which might be a result of various factors such particle size, gel point, and fibril compactness. For 60% fines, a 1 min redispersion suffices to achieve suspensions with stability similar to the original suspension, while we recommend a 5-min redispersion for 90% fines samples dewatered above 15 wt% CNFs to attain stable suspensions. This difference in redispersion time requirements could be attributed to higher hydrogen bonding among fibrils in samples with a higher fines percentage. Therefore, we recommend that the highest solid wt% achievable through ultrasonic dewatering while still maintaining successful redispersion to original suspension stabilities for both fines percentages is 35 wt% CNFs.

We also employed UV–vis transmittance spectroscopy to detect agglomerations in redispersed suspensions. The transmittance values for both 60% and 90% fines samples were found to be similar to their respective original suspensions, thereby suggesting that no significant agglomeration was triggered upon dewatering and subsequent redispersion of these samples.

Author contributions UR performed experiments, analyzed results and wrote the manuscript. RM and SB provided intellectual guidance. All authors reviewed the manuscript.

Funding The authors would like to acknowledge the support from Renewable Bioproducts Institute and the Brook Byers Institute for Sustainable Systems at Georgia Tech, Atlanta, USA. The authors would also like to thank the team from the Process Development Centre at University of Maine, Dr. Colleen Walker, Dr. Douglas Bousfield and Donna A. Johnson, for providing samples.

Data availability Additional information is provided as supplementary information.

Declarations

Conflict of interest The authors declare no conflict of interest.

Consent for publication The authors consent for publication by the journal.

References

Chen Y, Zhang L, Yang Y et al (2021) Recent progress on nanocellulose aerogels: preparation, modification, composite fabrication, applications. Adv Mater. https://doi.org/10.1002/adma.202005569

Colson J, Bauer W, Mayr M et al (2016) Morphology and rheology of cellulose nanofibrils derived from mixtures of pulp fibres and papermaking fines. Cellulose 23:2439–2448. https://doi.org/10.1007/s10570-016-0987-x

de Assis CA, Iglesias MC, Bilodeau M et al (2018) Cellulose micro- and nanofibrils (CMNF) manufacturing-financial and risk assessment. Biofuels Bioprod Biorefin 12:251–264. https://doi.org/10.1002/bbb.1835

Déléris I, Wallecan J (2017) Relationship between processing history and functionality recovery after rehydration of dried cellulose-based suspensions: a critical review. Adv Colloid Interface Sci 246:1–12. https://doi.org/10.1016/j.cis.2017.06.013

Ghasemi S (2019) Cellulose nanofibrils (CNF) for textile applications: production of neat CNF filaments and reinforcement of natural fiber yarns. University of Maine.

He M, Yang G, Cho B-U et al (2017) Effects of addition method and fibrillation degree of cellulose nanofibrils on furnish drainability and paper properties. Cellulose 24:5657–5669. https://doi.org/10.1007/s10570-017-1495-3

ISO (2012) ISO 10376, Pulps—Determination of mass fraction of fines

ISO (2014) ISO 16065-2 pulps: determination of fiber length by automated optical analysis–part, vol 2. Unpolarized light method

Jang MJ, Park B-D, Kweon H et al (2015) Preparation, structure, and properties of cellulose nanofibril/silk sericin composite film. Int J Ind Entomol 31:1–6. https://doi.org/10.7852/IJIE.2015.31.1.1

Johnson D, Papadis M, Bilodeau M et al (2016) Effects of cellulosic nanofibrils on papermaking properties of fine papers. TJ 15:395–402. https://doi.org/10.32964/TJ15.6.395

Kelly PV, Gardner DJ, Gramlich WM (2021) Optimizing lignocellulosic nanofibril dimensions and morphology by mechanical refining for enhanced adhesion. Carbohydr Polym 273:118566. https://doi.org/10.1016/j.carbpol.2021.118566

Lai PC, Yu SS (2021) Cationic cellulose nanocrystals-based nanocomposite hydrogels: achieving 3d printable capacitive sensors with high transparency and mechanical strength. Polymers 13:1–17. https://doi.org/10.3390/polym13050688

Moon RJ, Martini A, Nairn J et al (2011) Cellulose nanomaterials review: structure, properties and nanocomposites. Chem Soc Rev 40:3941. https://doi.org/10.1039/c0cs00108b

Miller T, Kramer C, Fisher A (2015) Bandwidth study on energy use and potential energy saving opportunities in U.S. pulp and paper manufacturing. US Department of Energy

Moon RJ, Hensdal CL, Beck S et al (2023) Setting priorities in CNF particle size measurement: what is needed vs.

what is feasible. TJ 22:116–137. https://doi.org/10.32964/TJ22.2.116

Nigmatullin R, Johns MA, Muñoz-García JC et al (2020) Hydrophobization of cellulose nanocrystals for aqueous colloidal suspensions and gels. Biomacromol 21:1812–1823. https://doi.org/10.1021/acs.biomac.9b01721

Patel DK, Dutta SD, Lim KT (2019) Nanocellulose-based polymer hybrids and their emerging applications in biomedical engineering and water purification. RSC Adv 9:19143–19162. https://doi.org/10.1039/c9ra03261d

Posada P, Velásquez-Cock J, Gómez-Hoyos C et al (2020) Drying and redispersion of plant cellulose nanofibers for industrial applications: a review. Cellulose 27:10649–10670. https://doi.org/10.1007/s10570-020-03348-7

Rebouillat S, Pla F (2013) State of the art manufacturing and engineering of nanocellulose: a review of available data and industrial applications. J Biomater Nanobiotechnol 04:165–188. https://doi.org/10.4236/jbnb.2013.42022

Raj P, Mayahi A, Lahtinen P et al (2016) Gel point as a measure of cellulose nanofibre quality and feedstock development with mechanical energy. Cellulose 23:3051–3064. https://doi.org/10.1007/s10570-016-1039-2

Ringania U, Harrison J, Moon RJ, Bhamla MS (2022) Dewatering of cellulose nanofibrils using ultrasound. Cellulose 29:5575–5591. https://doi.org/10.1007/s10570-022-04626-2

Stelte W, Sanadi AR (2009) Preparation and characterization of cellulose nanofibers from two commercial hardwood and softwood pulps. Ind Eng Chem Res 48:11211–11219. https://doi.org/10.1021/ie9011672

UMaine The Process development Center (2021) https://umaine.edu/pdc/nanocellulose/. Accessed 7 July 2021

Varanasi S, He R, Batchelor W (2013) Estimation of cellulose nanofibre aspect ratio from measurements of fibre suspension gel point. Cellulose 20:1885–1896. https://doi.org/10.1007/s10570-013-9972-9

Xu Y, Xu Y, Chen H et al (2022) Redispersion of dried plant nanocellulose: a review. Carbohydr Polym 294:119830. https://doi.org/10.1016/j.carbpol.2022.119830

Zhou X, Guo Y, Zhao F, Yu G (2019) Hydrogels as an emerging material platform for solar water purification. Acc Chem Res 52:3244–3253. https://doi.org/10.1021/acs.accounts.9b00455

Zambrano F, Starkey H, Wang Y et al (2020) Using micro- and nanofibrillated cellulose as a means to reduce weight of paper products. Rev BioResour 15:4553–4590